Third International Conference on Energy, Materials, Applied Energetics and Pollution
ICEMAEP2016, October 30-31, 2016, Constantine,Algeria
M.KADJA, A.ZAATRI, Z.NEMOUCHI, R.BESSAIH, S.BENISSAAD and K. TALBI (Eds.)

NUMERICAL SIMULATION OF A NEW GAS-LIQUID SEPARATOR

Nabil Kharoua[1], Lyes Khezzar [2], Mohamed AlShehhi [3], Mahmoud Meribout[4]

[1]Mechanical Engineering Department, Petroleum Institute, Abu Dhabi, UAE, nkharoua@pi.ac.ae
[2] Mechanical Engineering Department, Petroleum Institute, Abu Dhabi, UAE, malshehhi@pi.ac.ae
[3]Mechanical Engineering Department, Petroleum Institute, Abu Dhabi, UAE, lkhezzar@pi.ac.ae
[4] Electrical Engineering Department, Petroleum Institute, Abu Dhabi, UAE, mmeribout@pi.ac.ae

ABSTRACT

The complex multiphase flow, in a new Gas-Liquid separator, was simulated using the SST k-ω and Eulerian-Eulerian models. The flow split was imposed in the simulations using Outflow boundary condition to mimic flow control in the real installation. Three cases were simulated to assess the effects of different flow split on the separator performance and internal flow.

It was found that balancing the oil-in-gas and gas-in-oil entrainments simultaneously is difficult to achieve. The flow split has no effect on the flow field upstream of the cone. Recirculation zones develop in the annular space downstream of the cone and plays a key role in the separator performance.

Key Words: Gas-Liquid separator, Swirling flow, Eulerian-Eulerian model.

1. INTRODUCTION

Gas-Liquid and Liquid-Liquid separators, based on centrifugal separation, are widely used in the oil industry. They have developed from simple cylinders with tangential inlets and outlets to more complex geometries including swirl generators and different internal parts (see review of [1]). Recently, a separator, with a cone at its centreline, was developed. The cone contains a passage for the gas while the liquid, ejected towards the outer wall and forming a thin layer, is collected downstream. The generated multiphase flow is characterised by a swirling stream interacting with a bluff body.

Plenty of work was done on swirling flows in pipes [2-5]. Unlike for single-phase swirling flows, the complex flows of gas-liquid mixtures undergoing a swirling effect is a new research area tackled recently by few researchers [6-8]. These studies yielded useful flow regime maps for gas-liquid swirling flows in different orientations. CFD studies related to the field, allowed to establish the best practice guidelines for a successful simulation of such complex flows [9-11]. Different degrees of accuracy could be reached depending on the complexity of the models used and the computational cost they engender. There was an agreement that the combination of RANS-based turbulence model with an Eulerian multiphase model can predict the main features of the flow however, details such as interface capture and poly-dispersity effects require combinations such as LES/Eulerian/Lagrangian or DNS/Eulerian/Lagrangian models. Multiphase swirling pipe flows can become more complex when solid bodies are present inside the pipe. For example hydrocyclones are usually equipped with a rod placed at the centreline to avoid the formation of an undesirable air core [12-13]. For some applications, a cylinder is placed at the centreline with one side connected to the outlet of the lighter phase. It is called vortex finder [14]. Another example is the Ranque-Hilsch Vortex Tube [15]. Although detailed studies on the interaction of the swirling flow with bluff bodies are scarce, it can be concluded that the use of solid bodies at the centreline of gas-liquid separators has two main advantages; namely: altering the core flow totally or partially depending on the application and reducing the passage section to accelerate the flow and avoid a rapid swirl decay.

In the present work, the flow in a new Gas-Liquid separator is simulated using the Shear Stress Transport SST k-ω and Eulerian-Eulerian models. The fraction of the total flow is prescribed at each outlet mimicking the action of the control valves. The simulation approach is presented in the next section followed by the discussion of the results and the main conclusions from this work.

2. NUMERICAL APPROACH

2.1. Mathematical and numerical modeling assumptions

The Eulerian-Eulerian multiphase model solves individual continuity and momentum equations for each phase. The flow is assumed three-dimensional, unsteady and incompressible.

The continuity equation is solved for each secondary phase q to obtain the corresponding volume fraction. The volume fraction of the primary phase is calculated based on the assumption that the volume fractions of all the phases should sum to unity in each computational cell. The SST k-ω for the mixture is used to account for turbulence effects in the multiphase flow. More details about the models used can be found in ANSYS FLUENT Theory Guide [16].

2.2. Geometry and computational mesh

The geometry of the separator and computational mesh are illustrated in Figure 1

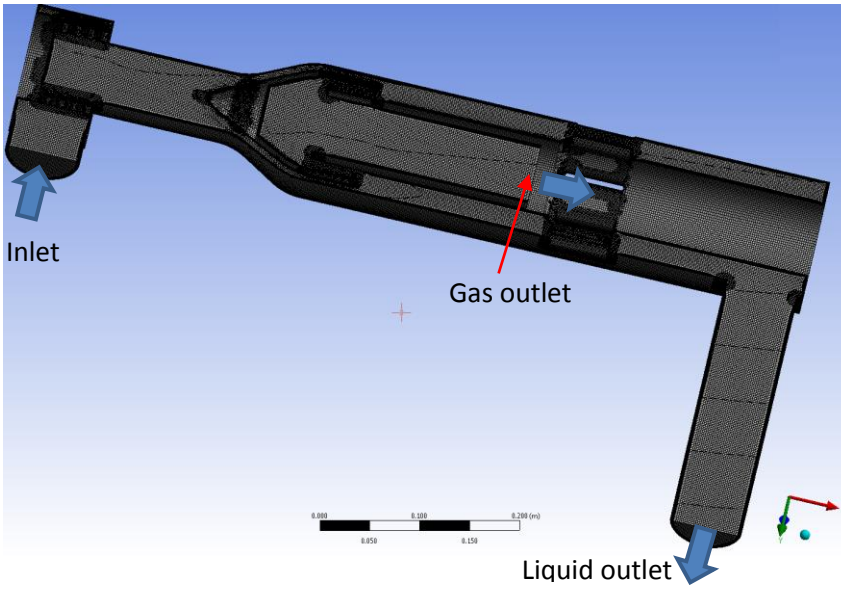

FIGURE 1. Geometry and mesh

The separator has one inlet and two outlets as indicated in the figure. The computational domain was divided into 5.2 million hexahedral cells. A finer, gradually enlarged, layer of cells was generated near the walls to account for boundary layers. The outlets were slightly prolonged to avoid the possible undesirable numerical effects of the Outflow boundary condition imposed at the outlets.

2.3. Boundary conditions

Table 1 summarizes the boundary conditions imposed at the inlet and the two outlets of the separator. At the inlet, the phase velocity and volume fraction were prescribed in addition to the turbulence intensity assumed to be equal to 5%. An Outflow boundary condition was imposed at the two outlets of the separator. It allows to impose the appropriate flow split independently of the phase concentration by prescribing the volumetric fraction of the total flow that leaves from each

outlet. At the walls, no slip condition was used for both phases. In addition, the turbulent kinetic energy and the specific dissipation rate are calculated, at the walls, using the standard wall function. The properties of the oil and gas phases are illustrated in Table 2.

Table 1: Boundary conditions

Case	Total flow rate (kg/s)	Inlet velocity (m/s)	Inlet volume Concentrations imposed		Total flow fraction at outlet (Flow split) Imposed	
			Oil (%)	Gas (%)	Oil outlet	Gas outlet
Case 1	6.23	10.49	15	85	0.17	0.83
Case 2	6.23	10.49	15	85	0.25	0.75
Case 3	6.23	10.49	15	85	0.5	0.5

Table 2: Phase properties

	Density (kg/m3)	Viscosity (kg/ms)
Oil	685.3055278	0.0003687
Gas	27.13706018	1.29593E-05

2.4. Numerical tools and simulation strategy.

The simulations started with no oil inside the computational domain. Simulations with gas only were conducted during 0.3 s of time to allow the single-phase flow to develop before the oil was injected at the inlet of the separator. Then, a transient period of approximately 0.5 s was necessary for the oil to reach the oil outlet. Finally, the average flow variables were calculated during a subsequent period longer than 1s. To mimic the flow split control, the flow fractions at the two outlets were varied to increase the flow rate at the oil outlet and decrease it at the gas outlet as shown in table 1. The purpose was to minimize the oil-in-gas entrainment.

3. RESULTS AND DISCUSSION

3.1. Performance of the separator

The performance of the separator is discussed based on the time-averaged phase concentration and pressure drop at the outlets. In addition, the time-averaged normal velocity of the mixture, at the outlets, is also reported. The corresponding results are summarized in table 3.

Cases 1-3 are intended to mimic the flow controller. It would have been ideal to automate the flow split control in the simulations. However, in ANSYS FLUENT, User Defined Functions UDFs cannot be applied to the Outflow boundary condition used. Thus, it was decided to simulate few cases with a constant flow split for each. When the flow split changes from 0.17-0.83 (case 1) to 0.5-0.5 (case 3), the mean volume fraction of oil at the gas outlet decreases from 2.7 % to a negligible value while the mean volume fraction of the gas at the oil outlet increases by about 72 %. Thus, controlling the flow split to minimize the amount of oil-in-gas will cause a consequent increase in the amount of gas-in-oil. On the other hand, the change in flow split, from case 1 to case 3, causes the flow to accelerate at the oil outlet with an increasing pressure drop and decelerate at the gas outlet with a decreasing pressure drop.

Table 3: Summary of the results at the outlets of the separator

Case	Mean volume fraction at outlet				Pressure drop (Pa) from in let towards		Normal velocity component (m/s)	
	Oil outlet		Gas outlet					
	Oil	Gas	Oil	Gas	Oil outlet	Gas outlet	Oil outlet	Gas outlet
Case 1	0.82	0.18	0.027	0.973	40659.48	50128.33	1.86	8.84

Case 2	0.66	0.34	0.007	0.993	44360.63	47541.21	2.78	8.18
Case 3	0.36	0.64	0.00003	0.99997	48662.38	44689.28	5.53	5.58

3.2. Velocity field

Figure 2 illustrates the mean velocity of the gas phase inside the separator which captures the regions where the flow accelerates. It is clear that the swirl cage generates an accelerated swirling flow with a low-velocity core. Upstream of the cone and in the annular space, the flow is identical for case 1-3 because the inflow is the same.

The interesting phenomenon is the different flow field downstream of the annular space between the cone and the external wall of the separator.

In fact, the flow split dictates the flow behavior in the two regions of the separator leading to the oil and gas outlets, respectively. The acceleration of the flow towards the oil-outlet side in conjunction with a deceleration in the gas-outlet side (from case 1 to case 3), promotes the minimization of oil-in-gas but increases the gas-in-oil entrainment as seen in Table 3. The inverse is also valid. Thus, minimizing the oil-in-gas and gas-in-oil entrainments cannot be achieved simultaneously.

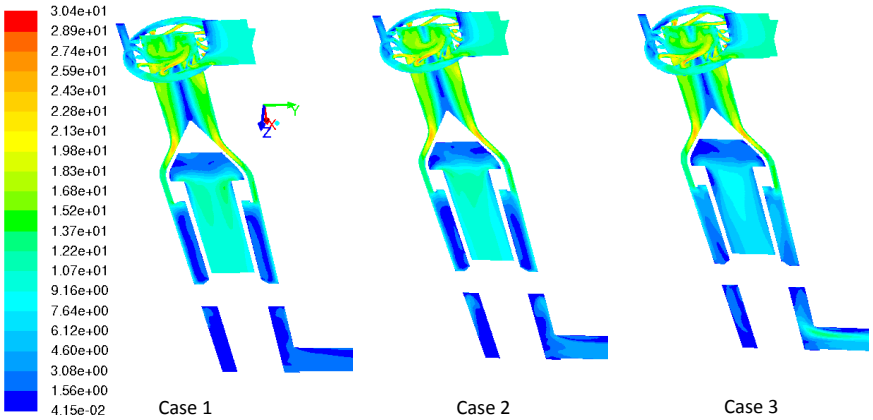

FIGURE 2. Contours of the mean gas velocity at z=0 and a surface crossing the inlet region

Figure 3 shows the direction of the flow in the two annular spaces surrounding the central cone using streamtraces. The oil volume fraction is superimposed on the streamtraces. Apart from case 3, a recirculation zone develops within the large annular space with an axis situated close to the bottom end of the large annular space. This recirculation zone is present for cases 1 and 2.

The recirculation zone promotes the oil-in-gas entrainment in addition to the deviated stream immediately at the entrance of the cone which is located at the step expansion between the two annular spaces. The absence of the recirculation zone for case 3 justifies the negligible oil-in-gas entrainment as shown in Table 3. The flow towards the oil outlet increased considerably and generated a small recirculation zone at the entrance of the cone as illustrated in Figure 3. This is similar to the recirculation zones generated by flow in junctions.

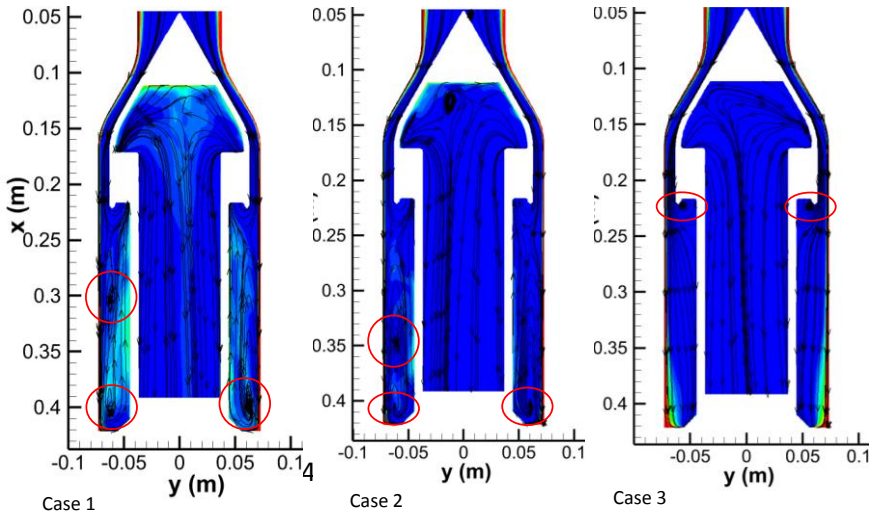

FIGURE 3. Streamtraces superimposed on oil volume fraction within the cone region

Profiles of the mean tangential gas velocity are plotted in Figure 4. The profiles illustrate the swirl decay from a position within the inlet region to a final position close to the oil outlet. At line 1, the profiles is asymmetrical because of the inlet configuration. Actually, the closest are the small passages from the main inlet the stronger is the flow rate through them. However, the profiles tends to be more symmetric for lines 2-4 downstream of the inlet region. Profiles 3 and 4 show the effect of the cone tip at the centerline where zero velocity turns to become wall-affected region at both sides of the cone. In the annular subsequent spaces (lines 5-8) the tangential velocity is damped considerably under the effect of friction tending towards a wall jet when approaching the oil outlet.

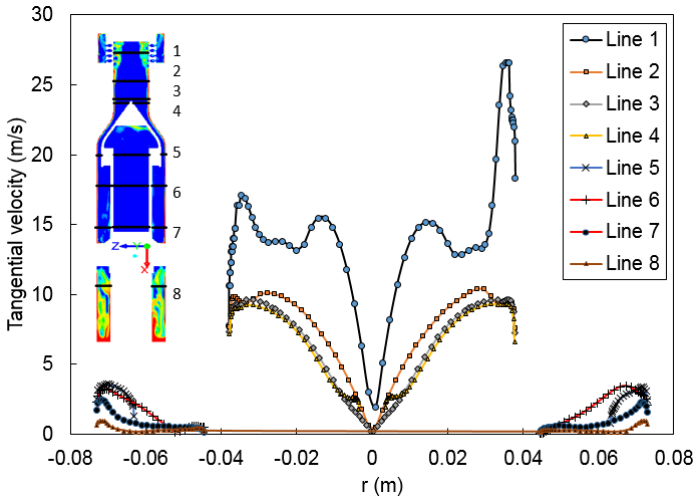

FIGURE 4. Mean gas tangential velocity at different axial positions

3.3. Phase distribution

The time-averaged oil volume fraction distribution, in a plane z=0, is depicted in Figure 5. The oil separates inside the swirl cage. A first thick layer, with low volume fraction, is seen at the top of the separator. In the small pipe segment upstream of the cone, the oil layer becomes more concentrated and thinner under the effect of the centrifugal separation ejecting the oil droplets towards the outer wall of the pipe segment. The thin oil layer persists in the two subsequent annular spaces. In the bottom part, downstream of the large annular space towards the oil outlet, the oil layer disappear because the swirling flow vanishes under the effect of the straight guiding vanes causing dispersion or stratification of the oil depending on the flow split imposed . A clear stratification is seen for case 3. Inside the cone, traces of oil can be seen for cases 1 and 2. Indeed, Table 3 shows that case 1 yields a relatively high oil volume fraction at the gas outlet confirming the behavior described in Figure 5.

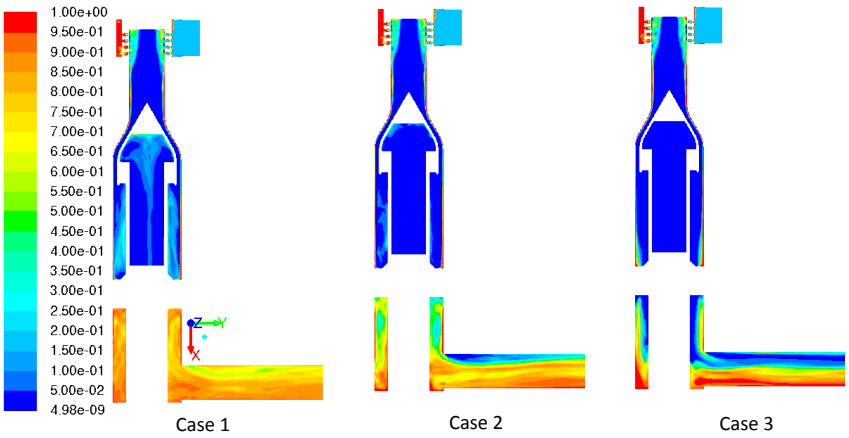

FIGURE 5. Space-time plots of pressure fluctuations at different positions x/H upstream of the impingement wall

4. CONCLUSIONS

Numerical simulations were conducted using the SST k-ω and Eulerian-Eulerian models to study the complex multiphase flow inside a new separator. The flow split is a crucial parameter to control the performance of the separator and it was imposed in the simulations using Outflow boundary condition. Three cases were considered corresponding to a constant inflow with different flow splits.

The pressure drop and outlet velocity increased with the increase of the outflow in one outlet when the flow split was changed. Also, it was seen that minimizing the oil-in-gas entrainment in the gas outlet side causes the increase of the gas-in-oil entrainment in the oil outlet side under the effect of flow split control. The flow filed is identical upstream of the cone while the effects of the flow split imposed appear downstream of the cone. A recirculation zone develops in the annular space downstream of the cone and plays a key role in the separator performance. It is generated under the effect of the higher flow rate towards the gas outlet and disappears when the flow rate towards the oil outlet tends to be equal or higher. Similarly to the flow filed, the phase distribution is identical upstream of the cone and depends on the flow split downstream of the cone.

REFERENCES

[1] N. Kharoua, L. Khezzar, and Z. Nemouchi, Hydrocyclones for De-Oiling Applications: A Review, *Petroleum Science and Technology*, 28(7), 738-755, 2010.
[2] O. Kitoh, Experimental study of turbulent swirling flow in a straight pipe, *Journal of Fluid Mechanics*, 225, 445-479, 1991.
[3] W. Steenbergen, Turbulent Pipe Flow with Swirl. PhD thesis, Technische Universiteit Eindhoven, Netherlands, 1995.
[4] A.F. Moene, Swirling pipe flow with axial strain Experiment and Large Eddy Simulation. PhD thesis. Technische Universiteit Eindhoven, Netherlands, 2003.
[5] A. Javadi, and H. Nilsson, Time-accurate Numerical Simulations of Swirling Flow with Rotor-stator Interaction, *Flow Turbulence Combust.*, 95(4), 755-774, 2015.
[6] H. Shakutsui, T. Suzuki, S. Takagaki, K. Yamashita, and K. Hayashi, Flow patterns in swirling gas-liquid two-phase flow in a vertical pipe, 7th International Conference on Multiphase Flow ICMF 2010. May 30–June 4,Tampa FL, USA, 2010.
[7] S. Wang, Y. Rao, Y. Wu, and X. Wang, Experimental two phase spiral flow in horizontal pipe, *China Pet. Process Pe*., 14, 24-32, 2012.
[8] B. Liu, and B. Bai, Swirl decay in the gas–liquid two-phase swirling flow inside a circular straight pipe, *Experimental Thermal and Fluid Science*, 68, 187-195, 2015.
[9] M. Narasimha, M. Brennan, and P.N. Holtham, A review of CFD modelling for performance predictions of hydrocyclones, *Engineering Applications of Computational Fluid Dynamics*, 1, 71-87, 2007.
[10] K. Karimi, G. Akdogan, S.M. Bradshaw, and A. Mainz, Numerical modelling of air core in hydrocyclones, Ninth International Conference on CFD in the Minerals and Process Industries CSIRO, December 10-12, Melbourne, Australia, 2012.
[11] F. Zonta, C. Marchioli, and A. Soldati, Particle and droplet deposition in turbulent swirled pipe flow, *International Journal of Multiphase Flow*, 56, 172-183, 2013.
[12] W.K. Evans, A. Suksangpanomrung, and A.F. Nowakowski, The simulation of the flow within a hydrocyclone operating with an air core and with an inserted metal rod, *Chemical Engineering Journal*, 143, 51-61, 2008.

[13] R. Sripriya, M.D. Kaulaskar, S. Chakraborty, and B.C. Meikap, Studies on the performance of a hydrocyclone and modeling for flow characterization in presence and absence of air core, *Chemical Engineering Science*, 62, 6391-6402, 2007.
[14] P.V. Cueille, E.S. Rosa, G. Sanchez-Soto, M.N. Noui-Mehidi, and M. Rivero, Swirl tubes as an in-line gas-liquid separator, Fifth International Conference on Computational Fluid Dynamics in the Process Industries, December 13-15, Melbourne, Australia. 2006.
[15] R. Liew, Droplet behaviour and thermal separation in Ranque-Hilsch vortex tubes. PhD thesis, Technische Universiteit Eindhoven, Netherlands, 2013.
[16] ANSYS Inc. Fluent User Guide and Fluent Theory Guide, 2015, version 16.2.